HHS Public Access

Author manuscript

Neuropharmacology. Author manuscript; available in PMC 2018 September 01.

Published in final edited form as:

Neuropharmacology. 2017 September 01; 123: 88–99. doi:10.1016/j.neuropharm.2017.05.019.

A novel iron (II) preferring dopamine agonist chelator D-607 significantly suppresses α-Syn- and MPTP-induced toxicities *in vivo*

Banibrata Das[1], **Subramanian Rajagopalan**[3], **Gnanada S. Joshi**[2], **Liping Xu**[1], **Dan Luo**[1], **Julie K. Andersen**[3], **Sokol V. Todi**[2], and **Aloke K. Dutta**[1,*]

[1]Department of Pharmaceutical Sciences, Wayne State University, Detroit, MI 48202

[3]Buck Institute for Research on Aging, 8001 Redwood Blvd, Novato, CA 94945

[2]Department of Pharmacology, Wayne State University, Detroit, MI 48201

Abstract

Here, we report the characterization of a novel hybrid D_2/D_3 agonist and iron (II) specific chelator, **D-607,** as a multi-target-directed ligand against Parkinson's disease (PD). In our previously published report, we showed that **D-607** is a potent agonist of dopamine (DA) D_2/D_3 receptors, exhibits efficacy in a reserpinized PD animal model and preferentially chelates to iron (II). As further evidence of its potential as a neuroprotective agent in PD, the present study reveals **D-607** to be protective in neuronal PC12 cells against 6-OHDA toxicity. In an *in vivo Drosophila melanogaster* model expressing a disease-causing variant of α-synuclein (α-Syn) protein in fly eyes, the compound was found to significantly suppress toxicity compared to controls, concomitant with reduced levels of aggregated α-Syn. Furthermore, **D-607** was able to rescue DAergic neurons from MPTP toxicity in mice, a well-known PD neurotoxicity model, following both sub-chronic and chronic MPTP administration. Mechanistic studies indicated that possible protection of mitochondria, up-regulation of hypoxia-inducible factor, reduction in formation of α-Syn aggregates and antioxidant activity may underlie the observed neuroprotection effects. These observations strongly suggest that **D-607** has potential as a promising multifunctional lead molecule for viable symptomatic and disease-modifying therapy for PD.

Graphical abstract

Corresponding Author: Aloke K. Dutta, Ph.D., Department of Pharmaceutical Sciences, Eugene Applebaum College of Pharmacy & Health Sciences, Wayne State University, Detroit, MI 48202, Tel: 1-313-577-1064, Fax: 1-313-577-2033, adutta@wayne.edu.

Declaration of interests: The authors have no conflicts of interest concerning this work.

Appendix A. Supplementary data: Supplementary data related to this article can be found at.

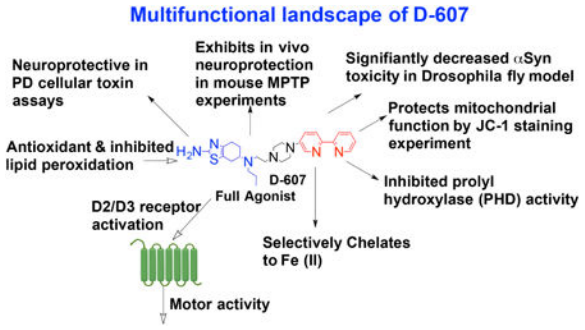

Keywords

Multifunctional dopamine agonist; α-synuclein; MPTP; 6-OHDA; neuroprotection; Parkinson's disease; *Drosophila*

1. Introduction

Parkinson's disease (PD) is a major neurodegenerative disorder that affects 1-2% of the population over 60 years of age. PD causes profound motor impairments including tremors at rest, rigidity, bradykinesia, and postural instability along with non-motor symptoms such as autonomic, cognitive and psychiatric problems (Olanow et al., 2009; Schapira and Olanow, 2004). PD is a multifactorial disease that includes, but is not limited to, oxidative stress, mitochondrial dysfunction, inflammation and aberrant protein aggregation (Dawson and Dawson, 2003; Dunnett and Bjorklund, 1999). Higher level of iron in the nigral area in early stages of PD progression has been reported in numerous publications (Belaidi and Bush, 2016; Gerlach et al., 2006; Oakley et al., 2007), and has also been confirmed by magnetic resonance imaging (Gorell et al., 1995) and ultrasound studies (Berg, 2009). The proposed pathogenic mechanisms for iron-mediated neuronal degeneration involve increased oxidative stress, owing to the interaction between intracellular ferrous iron and hydrogen peroxide (H_2O_2) in the Fenton reaction to generate hydroxyl free radicals (Zecca et al., 2004), and may also cause aggregation of α-synuclein (α-Syn) protein to form toxic oligomers (Bharathi et al., 2007; Ostrerova-Golts et al., 2000). The aggregation of α-Syn protein has been linked to the pathogenesis of PD and Dementia with Lewy bodies (DLB) (Olanow and Tatton, 1999; Spillantini et al., 1997). In addition, iron and other metals have been implicated in aggregation of α-Syn (Danzer et al., 2009; Finkelstein et al., 2016; Lei et al., 2015; Uversky et al., 2001). Metals, especially iron, cause fibrilization of α-Syn either via disruption of the interaction between the N- and C-terminal regions of α-Syn or by metal-catalyzed oxidation (MCO) of α-Syn (Cole, 2008). In a recent experiment, an iron chelator compound, clioquinol, has been shown to be effective in improving cognitive and motor function in α-Syn transgenic mice (Finkelstein et al., 2016). Therefore, the critical cross talk between iron accumulation, α-Syn aggregation and neurodegeneration suggests that iron chelation is an attractive therapeutic strategy for potential use against PD progression (Li et al., 2011).

The first pharmacological treatment for PD, L-dopa, when given with a peripheral dopamine (DA) decarboxylase inhibitor, dramatically improves the symptoms of the disease by producing DA in DA-depleted neurons (Birkmayer and Hornykiewicz, 2001; Cotzias et al., 1969). However, long-term use of L-dopa gives rise to motor fluctuations with dyskinesias and a decrease in duration of response to a given L-dopa dose (Marsden and Parkes, 1976). Importantly, L-dopa alleviates only the symptoms without affecting the course of disease progression (Schapira et al., 2005). As of now, no neuroprotective drugs have been identified or approved by the FDA for the treatment of PD. The overall goal of our research is to develop orally active multifunctional treatment agents to address both symptomatic (relieving motor dysfunction) and disease-modifying neuroprotective effects to slow or stop the progression of the disease (Das et al., 2015; Ghosh et al., 2010; Li et al., 2010; Modi et al., 2014; Santra et al., 2013; Shah et al., 2014). A number of iron chelators have been employed in the preclinical and clinical studies of PD (Devos et al., 2014; Grolez et al., 2015). One such chelator, deferiprone, has shown promising results in a recently completed 12-month clinical trial in early-stage PD patients (Devos et al., 2014), indicating the potential application of suitable iron chelators in disease modification. Additionally, another iron chelator clioquinol, exhibited neuroprotection following both MPTP (1-methyl-4-phenyl-1,2,3,6-tetrahydropyridine) administration (Kaur et al., 2003) and in a transgenic α-Syn mouse model (Finkelstein et al., 2016).

In our effort to develop multifunctional symptomatic and disease modifying drugs for PD, we report here the pharmacological characterization of a novel, multifunctional compound, termed **D-607** (Fig. 1) based on our hybrid drug design template (Das et al., 2017; Dutta et al., 2004). In this molecule, a D_2/D_3 agonist moiety is linked to a bipyridyl moiety, a known iron-chelating agent that has preferential affinity for Fe^{2+} (Breuer et al., 1995; Cabantchik et al., 1996; Romeo et al., 2001). The presence of a bipyridyl fragment is highly significant due to the fact that the ratio of Fe^{3+}:Fe^{2+} from 2:1 in normal subjects is shifted to 1:2 in PD patients (Weinreb et al., 2013). Iron in the Fe^{2+} state can potentially participate in the Fenton reaction to generate reactive oxygen species (Rouault and Cooperman, 2006). Thus, a Fe^{2+} preferring chelator should provide greater beneficial effect against neurodegeneration. The lead molecule, **D-607**, not only exhibited potent *in vivo* activity in a PD animal model but also displayed neuroprotection effect in a cellular model which was attributed to preferential complexing with Fe^{2+} (Das et al., 2017). Moreover, the compound was efficacious in significantly reducing lipid peroxidation induced by Fe^{2+} *in vitro* delineating its antioxidant property (Das et al., 2017).

Here, we provide a detailed biological characterization of **D-607** to demonstrate its potent multifunctional neuroprotection properties both *in vitro* and *in vivo*. Our *in vitro* result indicates strong protection effect of **D-607** in PC12 cells from toxicity associated with 6-OHDA, a cellular PD model. In a highly relevant *in vivo* experiment involving a validated PD *Drosophila* model that expresses a pathogenic, mutant variant of α-Syn protein in fly eyes, the test compound is shown to have significant protective activity. Moreover, in an *in vivo* study using the well-characterized MPTP administration mouse model of PD, the compound was found to be significantly neuroprotective under both sub-chronic and chronic administration of the toxin (Przedborski et al., 2000; Przedborski et al., 2004). Additional

mechanistic studies were carried out to support our neuroprotection data. In addition to symptomatic benefit, this multi-functional drug should also provide a degree of neuroprotection over the course of treatment, the latter endowing the compound with disease-modifying capabilities.

2. Materials and Methods

2.1. Synthesis of D-607

D-607 (Fig. 1) was synthesized by a multistep synthesis process as described in our recent publication (Das et al., 2017).

2.2. Cell treatments with D-607 in the presence of 6-OHDA

PC12 cells (ATCC® CRL1721.1™, Manassas, VA, USA), a rat adrenal pheochromocytoma cell line, were cultured in T-75 flasks (Greiner Bio One, Frickenhausen, Germany) and maintained in RPMI 1640 medium supplemented with 10% heat-inactivated horse serum, 5% fetal bovine serum, 100 U/mL penicillin, and 100 μg/mL streptomycin at 37 °C in 95% air/5% CO_2. To assess the neuroprotective effects of the test compound, PC12 cells were pre-treated with different concentrations of **D-607** for 1 h and then the drug-containing media replaced with fresh culture media. Next, the cells were treated with 75 μM of 6-OHDA and finally incubated for another 24 h at 37°C in 5% CO_2. The control cells were treated with above media containing 0.01% DMSO only.

2.3. Measurement of cell viability

To determine the neuroprotective effects of the test compound from 6-OHDA mediated cell death, a quantitative colorimetric MTT assay was performed. PC12 cells were plated at 17,000 cells/well density in 100 μL media in 96 well plates for 24 h. Cells were treated with varying concentrations of **D-607** for 1 h followed by treatment with 75 μM of 6-OHDA as above. After incubation for 24 h, 5 mg/mL MTT solution (prepared in 1X PBS) was added to the cells (to a final concentration of 0.5 mg/mL) and the plates were further incubated at 37°C in 95% air/5% CO_2 atmosphere for 3–4 h to produce dark blue formazan crystals. Afterwards, the plates were centrifuged at 450 *g* for 10 min and the supernatants were carefully removed. Formazan crystals were dissolved by adding 100 μL of methanol:DMSO (1:1) mixture to each well and shaking at 25 °C for 30 mi n. Absorbance values were measured on a microplate reader (Biotek Epoch, Winooski, VT, USA) at 570 nm with background correction performed at 690 nm. Data from at least three experiments were analyzed using Graphpad software (Version 4, San Diego, CA, USA). Cell viability was defined as percentage reduction in absorbance compared to untreated controls.

2.4. Drosophila –based studies

Fly stocks were maintained in standard cornmeal food at 25°C in incubators maintained at ~60% humidity with diurnal cycle. For experiments, flies were crossed, raised and maintained at 30°C in standard cornmeal media. Once offspring eclosed from their pupal cases, they were switched to custom-made instant fly food (Genesee Scientific) containing either compound **D-607** at a final concentration of 0.1 or 0.25 mg/mL (in ultra-pure water) or Rifampicin (Sigma-Aldrich) at 1 mg/mL (in DMSO) and maintained at 30°C. Vehicle

control flies were maintained in the same type of food and the same conditions. At specific time points, fly heads were dissected for fluorescence imaging with an Olympus BX53 microscope equipped with a DP72 digital camera; fluorescence from each eye was quantified using the publicly available ImageJ software. Average retinal fluorescence for each treatment condition were calculated as previously described (Burr et al., 2014; Tsou et al., 2015a; Yedlapudi et al., 2016).

2.5. Native gels, western blotting and quantification

Post-fluorescence imaging, dissected fly heads were homogenized for use with the NativePAGE™ Novex® Bis-Tris Gel System (Life Technologies), as outlined by the manufacturer. Briefly, fly heads were homogenized using a Dunce homogenizer in 4X Native sample buffer. Lysates were centrifuged at 20,000 × g for 30 minutes at 4°C, the supernatant was loaded onto gradient 3-12% pre-cast native gels (BN1003BOX, Life Technologies) and proteins were electrophoresed in 1X light blue Cathode buffer containing 0.5% NativePAGE™ Cathode Additive (BN2002, Life Technologies). Proteins were transferred onto a PVDF membrane and detected using anti-α-Syn antibody (SC-7011-R, Santa Cruz, Biotechnology; 1:500). Anti-tubulin antibody (Sigma Aldrich; 1:5000) was used as loading control. Peroxidase conjugated secondary antibodies: goat anti-rabbit and goat anti-mouse (Jackson Immunoresearch; 1:5000) were used for visualization using chemiluminiscence (Clarity™ Western ECL Substrate, Bio-Rad) on a CCD-equipped VersaDoc 5000MP system (Bio-Rad). The signals from the western blots were quantified using the Quantity One Software (Bio-Rad) with global noise reduction and using non-saturated blots as described before (Blount et al., 2012; Blount et al., 2014; Tsou et al., 2015b; Winborn et al., 2008).

2.6. In vivo MPTP neuroprotection studies

Sub-chronic administration—12-week old male C57BL/6 mice (Jackson Labs, Bar Harbor, ME) used in this study were housed according to standard animal care protocols, kept on a 12 h light/dark cycle, and maintained in a pathogen-free environment in the Buck Institute vivarium. All experiments were approved by local IACUC review and conducted according to current NIH policies on the use of animals in research. The compound **D-607** was diluted to a final dose of 5 mg/kg dissolved in saline and administered intraperitoneally (i.p.) to mice once daily for 5 days; control animals received saline vehicle. On day 4, mice were co i.p.-injected with either saline vehicle or 20 mg/kg MPTP (Sigma-Aldrich), administered 12 h apart. **D-607** or vehicle was administered 30 min before each MPTP injection (Joyce et al., 2003).

Chronic administration—12-week old male C57BL/6 mice (Jackson Labs, Bar Harbor, ME) were used in this study. The test compound **D-607** was diluted to a final dose of 5 mg/kg dissolved in saline and administered intraperitoneally (i.p.) to mice once daily for 8 days while control animals received saline vehicle only. On day 4, mice were co i.p.-injected with either saline vehicle or 20 mg/kg MPTP (Sigma-Aldrich), administered 24 h apart for five more days. **D-607** or vehicle was administered 30 min before each MPTP injection.

2.7. HPLC assay of striatal dopamine levels

A subset of mice (n=4 per condition) were used for analysis of levels of striatal DA. Dissected striata (harvested 24 hours after the final MPTP injection) were sonicated and centrifuged in chilled 0.1 M perchloric acid (PCA, 100 μL/mg tissue). Supernatants were taken for measurements of dopamine by HPLC as described previously (Beal et al., 1992; Beal et al., 1990). Briefly, 15 μL supernatant was isocratically eluted through an 80 × 4.6 mm C18 column (ESA, Inc Chelmsford, MA) with a mobile phase containing 0.1 M LiH_2PO_4 (lithium dihydrogen phosphate), 0.85 mM 1-octanesulfonic acid and 10% (v/v) methanol. DA was detected via a 2-channel Coulochem II electrochemical detector (ESA, Inc. Chelmsford, MA). Concentrations of DA are expressed as nanograms per milligram protein. Protein concentrations of tissue homogenates were measured according to the Bio-Rad protein analyze protocol (Bio-Rad Laboratories, Hercules, CA) using a Perkin Elmer Bio Assay Reader (Norwalk, CT) and used to normalize striatal DA levels.

2.8. Stereological assessment of DAergic SNpc cell numbers

A subset of mice (n=8 per condition) were subjected to cardiac perfusion with PBS followed by 4% paraformaldehyde at day 7 following the final MPTP injection. Brains were removed, dehydrated in 30% sucrose, and sectioned at 20 μm. Immunohistochemistry was performed using antibody against tyrosine hydroxylase (1:1000 TH, Chemicon, Temecula, CA) followed by biotin-labeled secondary antibody and development using DAB (Vector Labs, Burlingame, CA) to immunostain dopaminergic neurons. TH-positive cells in the SNpc were counted stereologically using the optical fractionator method (Kaur et al., 2003). Sections were cut at a 40 μm thickness, and every 4th section was counted using a grid of 100×100 μm. TH staining was verified by Nissl staining (Pilati et al., 2008).

2.9. Analysis of in vitro mitochondrial membrane potential by JC-1 staining

PC12 cells were cultured in 96-well black plates in 100 μL of RPMI-1640 media in a CO_2 incubator overnight at 37°C. The cells were pretre ated with different concentrations of **D-607** (0.1, 1, 5, 10, 20 and 30 μM) for 1 h, following which media containing the compound was removed and the cells were treated with 75 μM of 6-OHDA for another 24 h. At the end of the experiment, JC-1 at a concentration of 2 μg/mL was added to the cells and incubated for 2 h in a CO_2 incubator at 37 °C. The cells were washed twice with serum-free media to eliminate background fluorescence. Finally, 100 μL of serum free media was added to the cells and the fluorescence was measured using the Synergy Hybrid H1 fluorescence microplate reader (BioTek). JC-1 J-aggregates display fluorescence with excitation and emission at 550 nm and 600 nm while JC-1 monomers exhibit excitation and emission at 485 nm and 535 nm, respectively. The ratio of fluorescence intensities of J-aggregates to monomers (Red/Green) was used as an indicator for mitochondrial health (Szelechowski et al., 2014).

2.10. JC-1 staining image by fluorescence microscopy

PC12 cells were cultured in 48-well plates in 500 μL of RPMI-1640 media in a CO_2 incubator overnight at 37 °C. The cells were pretr eated with different concentrations of **D-607** for 1 h followed by treatment with 75 μM of 6-OHDA for another 24 h according to

the procedure described above. Then the cells were treated with JC-1 at a concentration of 2 μg/mL and incubated for 2 h, after which they were washed twice with serum-free media to eliminate background fluorescence. Finally, 300 μL of serum free media was added to the cells. Healthy cells with predominant JC-1 J-aggregates were detected with fluorescence settings designed to detect rhodamine (Texas Red filter) and apoptotic or unhealthy cells with mainly JC-1 monomers were detected with settings designed to detect FITC (GFP filter). Images were taken at 20× magnification with EVOS™ FL Cell Imaging System (Advanced Microscopy Group, USA). Representative images from two different sets of experiments were taken.

2.11. Western blots of hypoxia-inducible factor (HIF) levels

PC12 cells in RPMI 1640 media were plated at 5.5×10^5 cells/well density in 6-well plates and they were allowed to adhere for 24 h. Then the cells were treated with varying concentrations of **D-607** for 1 h after which the media containing drug was removed followed by incubation in fresh RPMI media for another 24 h. Cells were washed twice in ice-cold PBS and lysed in RIPA buffer for 30 min at 4 °C. A total of 40 μg protein was separated on 8% SDS-polyacrylamide gels (SDS-PAGE) and transferred to the polyvinylidene difluoride (PVDF) membranes (Bio-Rad, Hercules, CA, USA). The membrane was blocked with 5% (w/v) nonfat dry milk in TBS-T for 1 h at room temperature. Afterwards, the blocked membrane was incubated overnight at 4 °C with anti-HIF-1 α antibody (Novus Biologicals, USA; catalog # NB100-105SS) at a dilution of 1:500 in 5% (w/v) nonfat dry milk in TBS-T. Blots were washed three times in TBS-T and incubated for 1 h at room temperature with HRP-conjugated anti-mouse secondary antibody (1:5,000) in 5% (w/v) nonfat dry milk in TBS-T. The image was visualized using ECL-Plus reagent (Perkin–Elmer, Waltham, MA, USA) and ImageQuant LAS 4000 imager (GE Healthcare Biosciences, Pittsburgh, PA, USA). Densitometric analysis was performed using ImageJ software.

2.12. Statistics

Two-tailed Student t-tests or ANOVA with Tukey's post-hoc correction were used to assess retinal eye degeneration in treatment versus control groups, as appropriate, and as indicated in figure legends. For multiple groups distributed normally, statistical significance was determined using one-way ANOVA following Tukey's multiple comparison as well as Dunnett's post hoc test. In all cases, $p < 0.05$ was considered as statistically significant.

3. Results

3.1. Cell culture-based neuroprotection study

We first explored the neuroprotective effect of **D-607** *in vitro* in PC12 cells against 6-OHDA-induced cytotoxicity. Treatment of PC12 cells with 6-OHDA for 24 h resulted in significant, dose-dependent neurotoxicity as indicated by a significant decrease (~ 50%) in cells exposed to 75 μM 6-OHDA; this concentration was used in subsequent *in vitro* experiments (also see Fig. 5a, Shah et al., 2014). The potential neuroprotective effect of **D-607** on 6-OHDA-induced toxicity was evaluated following pre-treatment with the drug. When cells were pre-treated with **D-607** for 1 h prior to exposure to 6-OHDA treatment for

24 h, this resulted in dose-dependent protection against neurotoxicity. The highest protective effect was obtained at a concentration of 5 μM where cell survival was increased by ~60% compared to 6-OHDA (75 μM) treatment alone (Fig. 2 and Supl. Fig. 1).

3.2. α-Syn-dependent toxicity in Drosophila

Compound **D-607** was next examined for its ability to suppress neurotoxicity associated with a disease-causing variant of α-Syn in the fruit fly *Drosophila melanogaster*. Expression of both wild type and mutant variants of α-Syn in the fruit fly leads to age-dependent neurotoxicity (Burr et al., 2014; Feany and Bender, 2000). We utilized a sensitive technique in order to detect and track degeneration in fly eyes when α-Syn is expressed in them. This method reports retinal degeneration by making use of membrane-targeted GFP, whose fluorescence diminishes as internal structures deteriorate and collapse (Burr et al., 2014; Tsou et al., 2015a; Yedlapudi et al., 2016).

Expression of α-Syn in fly eyes is toxic. As shown in Fig. 3A, expression of a mutated version of α-Syn (mutation A30P, linked to human disease; (Kruger et al., 1998)) in fly eyes causes loss of overall GFP fluorescence and increased mosaicism when α-Syn is expressed in them. Quantification of overall eye fluorescence highlights these findings. As reported in our recent publication, we used rifampicin, which has been shown to suppress α-Syn toxicity in cell models (Bi et al., 2013; Li et al., 2004), as a positive reference for suppression of α-Syn-dependent retinal toxicity (Yedlapudi et al., 2016). Flies were reared in media that did not contain the drug until the day when they eclosed from the pupal case. At that time, adults were switched to media containing rifampicin or its vehicle control (DMSO) for 21 days. As shown in Fig. 3B, flies fed rifampicin for 21 days showed increased GFP fluorescence significantly compared with flies that were fed the vehicle control, indicative of neuroprotection from α-Syn.

We then proceeded to examine the ability of **D-607** to suppress toxicity from α-Syn through this parameter. As with rifampicin, flies were reared on media without the drug, and were switched to media containing **D-607** or its vehicle (ultra-pure water) after they eclosed from the pupal case. Flies that were fed the iron chelator **D-607** showed a dose-dependent increase in GFP fluorescence compared with their vehicle-treated siblings (Fig. 3C). Collectively, these data indicate a protective role from **D-607** in this synucleinopathy model.

In order to evaluate a possible role of iron chelating effect in reduction of α-Syn induced toxicity, we tested compound **D-636**, a close analog of **D-607**. **D-636** is a potent dopamine agonist, but unlike **D-607**, it does not have iron chelating property. As shown in Supl. Fig. 2, **D-636** was unable to produce significant reduction of toxicity at the same dose and time point as to **D-607**. This suggests a role from iron chelation in enhancement of protection from toxicity of α-Syn by **D-607**.

To obtain additional insight into the manner in which compound **D-607** reduces α-Syn neurotoxicity in the *Drosophila* model, we utilized native gel analyses to examine levels of various α-Syn species. Representative results from these assays are shown in Fig. 4. As highlighted in Fig. 4, left portion, α-Syn migrates as a monomer and as multimeric species in native gels. Some α-Syn bands and smears are visible in lighter exposures, whereas

longer exposures are required to observe others. We show three different exposures from one of the experiments. To compare the monomeric and multimeric species of α-Syn in each lane (Fig. 4, right portion), we quantified the monomeric band (arrow), the entire multimeric smear (bracket), and the total α-Syn signal (monomer + multimer) for each band. Then, we determined the portion of monomeric and multimeric α-Syn for each lane, based on total α-Syn, and normalized those results to the monomeric and multimeric values for the vehicle-treated control. It is these results that are shown as histograms in Fig. 4.

Treatment of flies with **D-607** for 21 days at 0.1 or 0.25 mg/mL led to a mild, but statistically significant, increase in monomeric species concomitant with reduction in multimeric or aggregated α-Syn forms compared to vehicle-only control (Fig. 4). This increase in monomeric α-Syn species was found to coincide with reductions in toxicity from this protein (Fig. 3), supporting the notion that the compound protects against α-Syn-dependent degeneration in fly eyes via decreased levels in aggregated α-Syn species.

3.3. Neuroprotective effects of D-607 under conditions of systemic sub-chronic and chronic MPTP treatment in mouse

3.3.1. D-607 protects against MPTP-induced depletion of striatal DA content duringsub-chronic administration—Effect of pre-treatment with 5 mg/kg **D-607** for three days followed by two days co-treatment with MPTP (20 mg/kg, 12 h apart) resulted in significant protection against losses in DA levels compared to control MPTP alone. Specifically, while treatment with MPTP alone at a dose 20 mg/kg, 12 h apart resulted in a 75% depletion in striatal DA levels compared to controls, treatment with 5 mg/kg **D-607** significantly reduced this striatal DA depletion (~28% reduction in DA loss versus MPTP treatment alone ($p<0.001$, Fig. 5a).

3.3.2. D-607 protects against MPTP-induced depletion of striatal DA contentfollowing chronic administration—Effects of pre-treatment of 5 mg/kg **D-607** for 3 days followed by 5 days co-treatment with MPTP (20 mg/kg, 24 h apart) resulted in significant protection against losses in striatal DA levels. Specifically, treatment with MPTP alone resulted in 80% depletion in striatal DA levels compared to controls, while pre-reatment with **D-607** reversed this loss by ~32% (Fig. 6a).

3.3.3. D-607 protects against MPTP induced SNpc DAergic cell loss during sub-chronic administration—Treatment with MPTP using the above dosage regime for sub-chronic administration resulted in a significant loss (39%) of DAergic SNpc neurons compared to untreated controls. Pre-treatment with 5 mg/kg of **D-607** conferred a significant reduction (22%) against DAergic SNpc neuronal loss compared to MPTP-treated group ($p<0.001$, Fig. 5b).

3.3.4. D-607 protects against MPTP- induced SNpc DAergic cell loss during chronicadministration—Treatment with MPTP under chronic administration regiment led to loss of 40% DAergic SNpc neurons compared to untreated control while both pre-treatment and co-treatment with 5 mg/kg **D-607** resulted in significant reduction (21%) of this cell loss (Fig. 6b).

3.4. Mitochondria as a therapeutic target for PD

We next analyzed the ability of **D-607** to modulate downstream effects on mitochondrial dysfunction. For these studies, we utilized JC-1 staining in our 6-OHDA cellular PD model as an indicator of mitochondrial health (Wagner et al., 2008). The staining was done by lipophilic fluorescent cationic dye JC-1 as an indicator of mitochondrial membrane potential (MMP). JC-1 forms red fluorescent J-aggregates when MMP is maintained or restored, while it forms green fluorescent monomers in the presence of decreases in MMP. Pre-treatment with **D-607** led to an increase in the red/green ratio in a dose-dependent manner when compared to 6-OHDA treatment alone. **D-607** alone did not have an observable effect on the mitochondrial membrane potential except at a higher dosage (30 mM) (Fig. 7a). However, treatment with **D-607** was found to increase mitochondrial membrane potential compared to 6-OHDA alone in a concentration-dependent manner. The most significant increase was shown in a concentration range of 5-30 μM (Fig. 7b). These data were further corroborated via fluorescent microscopy demonstrating a decrease in numbers of J-aggregates (Fig. 8); however, **D-607** was able to reverse the effects caused by 6-OHDA as evidenced by increases in numbers of J-aggregates.

3.5. Inhibition of prolyl hydroxylase (PHD) and up-regulation of HIF by D-607

To further probe into possible mechanisms involved in neuroprotection elicited by **D-607**, we carried out a well characterized cell based assay evaluating effects of drug on HIF-1α levels as a surrogate for inhibition of iron-dependent prolyl hydroxylase activity (Callapina et al., 2005; Yeoh et al., 2013). It has been demonstrated that elevation of HIF-1α level as a result of inhibition of PHD prevents neuronal death and provides neuroprotection (Lee et al., 2009; Siddiq et al., 2005). PC12 cells were treated with **D-607** for 1 h following the same protocol we employed in our *in vitro* neuroprotection experiments. As shown in Fig. 9, we observe a significant dose-dependent increase in HIF-1α levels following treatment of PC12 cells with **D-607**.

4. Discussion

We recently demonstrated the development of bipyridine-based, hybrid D_2/D_3 ligands that exhibit potent agonist efficacy in GTPγS binding functional assays. Our previous iron binding study revealed far higher specificity for complex formation of **D-607** with Fe(II) compared to Fe(III). This study also indicated a neuroprotective effect of **D-607** in neuronal PC12 cells against iron (II)-induced cell death (Das et al., 2017). The fact that compound **D-607** was able to rescue these cells strongly indicated the ability of selective intracellular complexation of Fe(II) by the compound to reduce oxidative stress. This was further validated in a cell-based lipid peroxidation assay where pre-treatment with the compound was found to significantly reduce iron (II) induced lipid peroxidation. Our results also demonstrated **D-607** to be much more neuroprotective in this experimental model versus pramipexole and a 8-hydroxyquinoline-derived Fe(III) preferring dopamine agonist, thereby, reflecting contribution of the bipyridyl moiety in enhanced neuroprotection (Das et al., 2017).

In an *in vitro* 6-OHDA PD model, pre-treatment with different doses of **D-607** was able to restore cell viability to almost control levels (Fig. 2). 6-OHDA is a widely-used toxin that mimics the generation of oxidative stress observed in PD which induces neurotoxicity via its auto-oxidation and subsequent hydrogen peroxide generation (Blum et al., 2000; Soto-Otero et al., 2000). It is interesting and worth mentioning that only a single hour pre-treatment of **D-607** was sufficient to protect cells from this neurotoxin.

We next assessed the *in vivo* neuroprotection potential of this compound in a proteotoxicity *Drosophila* model in which mutant pathogenic α-Syn protein is expressed specifically in fly eyes to produce detectable and quantifiable toxicity. *Drosophila* has a proven track record as a model for human neurodegenerative diseases (Bonini and Fortini, 2003; Jaiswal et al., 2012). The fruit fly is a complex living organism with an intricate nervous system whose molecular pathways are closely related to human. We previously reported a method to examine retinal degeneration in this model (Burr et al., 2014). This GFP-based technique is sufficiently sensitive that it can report degeneration even before it is consistently and easily observed through histology or by observing external eye structures. We have successfully used this technique to describe retinal degeneration caused by various toxic neurodegenerative disease proteins and as a means to identify modifiers for them (Burr et al., 2014; Tsou et al., 2015a; Yedlapudi et al., 2016).

Our results showed that the compound rifampicin significantly protects fly eyes from mutant α-Syn-based toxicity compared to untreated control in a dose-dependent manner (Fig. 3, Panels B, C). This confirms previous results on the protective effect of rifampicin on neurotoxicity associated with α-Syn (Li et al., 2004). Treatment with **D-607** at two different doses was effective. The effect was dose dependent as the 0.25 mg/mL concentration was more efficacious in this regard (Fig. 3, Panel C). Our results also indicate disruption of the formation of toxic aggregates in this model in the presence of **D-607**. To investigate the mechanism of neuroprotection, we carried out western blot-based analyses of the ratio of α-Syn species in the absence or presence of drug. Reductions in aggregate formation were found coincident with reductions in neurodegeneration in this model (Fig. 4). Interestingly, a non-iron chelating dopamine agonist **D-636**, a close analog of **D-607**, did not exhibit significant protection against α-Syn toxicity under the same experimental condition (Supl. Fig. 2). This indicates a possible role of iron chelation in protection from toxicity.

To further establish the neuroprotective effects of **D-607** *in vivo*, we carried out additional studies utilizing the well-characterized MPTP administration mouse model. Systemic administration of MPTP produces selective destruction of DAergic SNpc neurons in both primates and rodents, resulting in an acute Parkinsonism phenotype (Lee et al., 2009; Przedborski et al., 2004). MPTP has been suggested to exert its neurotoxic effect via selective inhibition of mitochondrial complex I activity, resulting in both a reduction in ATP synthesis and accumulation of reactive oxygen species. MPTP therefore reproduces many of the hallmarks of PD-associated neurodegeneration. Results from these studies demonstrated **D-607** pre-treatment prevents losses in striatal dopamine levels and DAergic SNpc neurons elicited by either sub-chronic or chronic MPTP administration. Specifically, neurochemical striatal analysis showed significant protection (>28%) against MPTP-mediated losses in DA content in mice pretreated with **D-607** following sub-chronic MPTP administration

compared to MPTP-alone. Similarly, significant protection (>22%) against striatal DAergic cell loss as assessed by sterological cell counting was observed in the **D-607** pre-treatment group compared to MPTP treatment alone (Fig. 5b-c). In the case of chronic administration of MPTP, a robust neuroprotective effect was observed (>39%) in both striatal DA loss (Fig. 6a) and reductions in DAergic SN cell numbers (21%, Fig. 6b-c). As found by the other investigators, we do not see a significant impact from the treatment with **D-607** alone on the level of DA and TH cell counts (Joyce et al., 2003; Zou et al., 2000). **D-607** did not influence the metabolic conversion of MPTP to MPP^+ demonstrating that the conferred neuroprotection is not due to alterations in production of MPP^+ by the drug (Supl. Fig. 3).

Mechanisms associated with the neuroprotective effects of **D-607** from *in vitro* 6-OHDA and *in vivo* MPTP neurotoxicity may be partly explained by its ability to protect against oxidatively-induced alterations in mitochondrial dysfunction (Smiley et al., 1991; Szelechowski et al., 2014). For these studies, we employed the lipophilic fluorescent cationic dye JC-1 as an indicator of MMP. As mentioned above, maintenance or restoration of MMP is indicated by red fluorescence from J-aggregates, while it forms green fluorescent monomers when MMP decreases. Our results indicate that **D-607** is able to protect against losses in MMP induced by 6-OHDA (Fig. 7b). Both 6-OHDA and MPTP neurotoxicity are known to impair mitochondrial activity.

Inhibition of iron-dependent PHD activity, by preventing the ubiquitination and subsequent degradation of HIF-1α by the proteasome has been demonstrated to be neuroprotective against MPTP toxicity (Lee et al., 2009; Rajagopalan et al., 2016). Interestingly, deferoxamine, an iron chelator, has also been shown to up-regulate HIF-1α (Guo et al., 2016). We observed a clear induction of HIF-1α level by **D-607** in PC12 cells from concentration of drug as low as 100 nM to a higher concentration of 5 μM (Fig. 9). This result is in line with the known inhibitory activity of bipyridyl against PHD activity (Hales and Beattie, 1993; Ivan et al., 2002). The ability of **D-607**, acting in its capacity as an iron chelator, may also provide neuroprotection via its ability to inhibit PHD and up-regulate HIF-1α levels.

In summary, the absence of a disease-modifying drug for PD makes the development of multifunctional neuroprotective agents an important therapeutic strategy. To address this unmet medical need and the emerging role of redox-reactive iron (II) in PD, we previously developed a novel Fe^{2+} preferring DA agonist chelator, **D-607**. Here we show that the compound is neuroprotective in a cellular 6-OHDA induced neurotoxin PD model. In a unique *in vivo* fruit fly *Drosophila melanogaster* model specifically expressing a disease-causing variant of α-Syn protein in fly eyes, **D-607** was found to suppress retinal degeneration coinciding with reductions in toxic α-Syn aggregate formation. Finally, in a well-known mouse MPTP PD animal model, **D-607** was shown to confer significant neuroprotection against MPTP toxicity both in terms of losses in striatal DA levels and DAergic SNpc cell numbers following both sub-chronic and chronic MPTP administrations. Finally, we provide some possible mechanistic insights towards delineating the observed neuroprotective properties of the drug. Results from these studies, therefore, underpin the notion that a multifunctional drug like **D-607** has the potential not only to ameliorate motor

dysfunction in PD patients (Das et al., 2017), but also to modify disease progression by protecting DA neurons from neurotoxic insults.

Supplementary Material

Refer to Web version on PubMed Central for supplementary material.

Acknowledgments

This work was supported by National Institute of Neurological Disorders and Stroke/ National Institute of Health (NS047198, AKD) and Wayne State President Research Enhancement award (AKD, SVT). The *Drosophila* fly study was also partially supported by NIH/NINDS (NS086778, SVT).

References

Beal MF, Matson WR, Storey E, Milbury P, Ryan EA, Ogawa T, Bird ED. Kynurenic acid concentrations are reduced in Huntington's disease cerebral cortex. J Neurol Sci. 1992; 108:80–87. [PubMed: 1385624]

Beal MF, Matson WR, Swartz KJ, Gamache PH, Bird ED. Kynurenine pathway measurements in Huntington's disease striatum: evidence for reduced formation of kynurenic acid. J Neurochem. 1990; 55:1327–1339. [PubMed: 2144582]

Belaidi AA, Bush AI. Iron neurochemistry in Alzheimer's disease and Parkinson's disease: targets for therapeutics. J Neurochem. 2016; 139 Suppl 1:179–197.

Berg D. Transcranial ultrasound as a risk marker for Parkinson's disease. Mov Disord. 2009; 24 Suppl 1:S677–683. [PubMed: 19877199]

Bharathi, Indi SS, Rao KS. Copper- and iron-induced differential fibril formation in alpha-synuclein: TEM study. Neurosci Lett. 2007; 424:78–82. [PubMed: 17714865]

Bi W, Zhu L, Jing X, Liang Y, Tao E. Rifampicin and Parkinson's disease. Neurol Sci. 2013; 34:137–141. [PubMed: 22821065]

Birkmayer W, Hornykiewicz O. The effect of l-3,4-dihydroxyphenylalanine (= DOPA) on akinesia in parkinsonism. 1961. Wiener klinische Wochenschrift. 2001; 113:851–854. [PubMed: 11763859]

Blount JR, Burr AA, Denuc A, Marfany G, Todi SV. Ubiquitin-specific protease 25 functions in Endoplasmic Reticulum-associated degradation. PLoS One. 2012; 7:e36542. [PubMed: 22590560]

Blount JR, Tsou WL, Ristic G, Burr AA, Ouyang M, Galante H, Scaglione KM, Todi SV. Ubiquitin-binding site 2 of ataxin-3 prevents its proteasomal degradation by interacting with Rad23. Nat Commun. 2014; 5:4638. [PubMed: 25144244]

Blum D, Torch S, Nissou MF, Benabid AL, Verna JM. Extracellular toxicity of 6-hydroxydopamine on PC12 cells. Neurosci Lett. 2000; 283:193–196. [PubMed: 10754220]

Bonini NM, Fortini ME. Human neurodegenerative disease modeling using Drosophila. Annu Rev Neurosci. 2003; 26:627–656. [PubMed: 12704223]

Breuer W, Epsztejn S, Cabantchik ZI. Iron acquired from transferrin by K562 cells is delivered into a cytoplasmic pool of chelatable iron(II). J Biol Chem. 1995; 270:24209–24215. [PubMed: 7592626]

Burr AA, Tsou WL, Ristic G, Todi SV. Using membrane-targeted green fluorescent protein to monitor neurotoxic protein-dependent degeneration of Drosophila eyes. J Neurosci Res. 2014; 92:1100–1109. [PubMed: 24798551]

Cabantchik ZI, Glickstein H, Milgram P, Breuer W. A fluorescence assay for assessing chelation of intracellular iron in a membrane model system and in mammalian cells. Anal Biochem. 1996; 233:221–227. [PubMed: 8789722]

Callapina M, Zhou J, Schnitzer S, Metzen E, Lohr C, Deitmer JW, Brune B. Nitric oxide reverses desferrioxamine- and hypoxia-evoked HIF-1alpha accumulation--implications for prolyl hydroxylase activity and iron. Exp Cell Res. 2005; 306:274–284. [PubMed: 15878351]

Cole NB. Metal catalyzed oxidation of alpha-synuclein--a role for oligomerization in pathology? Curr Alzheimer Res. 2008; 5:599–606. [PubMed: 19075587]

Cotzias GC, Papavasiliou PS, Gellene R. Modification of Parkinsonism--chronic treatment with L-dopa. N Engl J Med. 1969; 280:337–345. [PubMed: 4178641]

Danzer KM, Krebs SK, Wolff M, Birk G, Hengerer B. Seeding induced by alpha-synuclein oligomers provides evidence for spreading of alpha-synuclein pathology. J Neurochem. 2009; 111:192–203. [PubMed: 19686384]

Das B, Kandegedara A, Xu L, Antonio T, Stemmler T, Reith ME, Dutta AK. A novel iron(II) preferring dopamine agonist chelator as potential symptomatic and neuroprotective therapeutic agent for Parkinson's disease. ACS Chem Neurosci. 2017; 8:723–730. [PubMed: 28106982]

Das B, Vedachalam S, Luo D, Antonio T, Reith ME, Dutta AK. Development of a highly potent D2/D3 agonist and a partial agonist from structure-activity relationship study of N(6)-(2-(4-(1H-Indol-5-yl)piperazin-1- yl)ethyl)-N(6)-propyl-4,5,6,7-tetrahydroben zo[d]thiazole-2,6-diamine analogues: Implication in the treatment of Parkinson's disease. J Med Chem. 2015; 58:9179–9195. [PubMed: 26555041]

Dawson TM, Dawson VL. Molecular pathways of neurodegeneration in Parkinson's disease. Science. 2003; 302:819–822. [PubMed: 14593166]

Devos D, Moreau C, Devedjian JC, Kluza J, Petrault M, Laloux C, Jonneaux A, Ryckewaert G, Garcon G, Rouaix N, Duhamel A, Jissendi P, Dujardin K, Auger F, Ravasi L, Hopes L, Grolez G, Firdaus W, Sablonniere B, Strubi-Vuillaume I, Zahr N, Destee A, Corvol JC, Poltl D, Leist M, Rose C, Defebvre L, Marchetti P, Cabantchik ZI, Bordet R. Targeting chelatable iron as a therapeutic modality in Parkinson's disease. Antioxid Redox Signal. 2014; 21:195–210. [PubMed: 24251381]

Dunnett SB, Bjorklund A. Prospects for new restorative and neuroprotective treatments in Parkinson's disease. Nature. 1999; 399:A32–39. [PubMed: 10392578]

Dutta AK, Venkataraman SK, Fei XS, Kolhatkar R, Zhang S, Reith ME. Synthesis and biological characterization of novel hybrid 7-[[2-(4-phenyl-piperazin-1-yl)-ethyl]-propyl-amino]-5,6,7,8-tetrahydro-naphthale n-2-ol and their heterocyclic bioisosteric analogues for dopamine D2 and D3 receptors. Bioorg Med Chem. 2004; 12:4361–4373. [PubMed: 15265488]

Feany MB, Bender WW. A Drosophila model of Parkinson's disease. Nature. 2000; 404:394–398. [PubMed: 10746727]

Finkelstein DI, Hare DJ, Billings JL, Sedjahtera A, Nurjono M, Arthofer E, George S, Culvenor JG, Bush AI, Adlard PA. Clioquinol Improves Cognitive, Motor Function, and Microanatomy of the Alpha-Synuclein hA53T Transgenic Mice. ACS Chem Neurosci. 2016; 7:119–129. [PubMed: 26481462]

Gerlach M, Double KL, Youdim MB, Riederer P. Potential sources of increased iron in the substantia nigra of parkinsonian patients. J Neural Transm Suppl. 2006:133–142.

Ghosh B, Antonio T, Reith ME, Dutta AK. Discovery of 4-(4-(2-((5-Hydroxy-1,2,3,4-tetrahydronaphthalen-2-yl)(propyl)amino)ethyl)piperaz in-1-yl)quinolin-8-ol and its analogues as highly potent dopamine D2/D3 agonists and as iron chelator: in vivo activity indicates potential application in symptomatic and neuroprotective therapy for Parkinson's disease. J Med Chem. 2010; 53:2114–2125. [PubMed: 20146482]

Gorell JM, Ordidge RJ, Brown GG, Deniau JC, Buderer NM, Helpern JA. Increased iron-related MRI contrast in the substantia nigra in Parkinson's disease. Neurology. 1995; 45:1138–1143. [PubMed: 7783878]

Grolez G, Moreau C, Sablonniere B, Garcon G, Devedjian JC, Meguig S, Gele P, Delmaire C, Bordet R, Defebvre L, Cabantchik IZ, Devos D. Ceruloplasmin activity and iron chelation treatment of patients with Parkinson's disease. BMC Neurol. 2015; 15:74. [PubMed: 25943368]

Guo C, Hao LJ, Yang ZH, Chai R, Zhang S, Gu Y, Gao HL, Zhong ML, Wang T, Li JY, Wang ZY. Deferoxamine-mediated up-regulation of HIF-1alpha prevents dopaminergic neuronal death via the activation of MAPK family proteins in MPTP-treated mice. Exp Neurol. 2016; 280:13–23. [PubMed: 26996132]

Hales NJ, Beattie JF. Novel inhibitors of prolyl 4-hydroxylase. 5. The intriguing structure-activity relationships seen with 2,2′-bipyridine and its 5,5′-dicarboxylic acid derivatives. J Med Chem. 1993; 36:3853–3858. [PubMed: 8254616]

Ivan M, Haberberger T, Gervasi DC, Michelson KS, Gunzler V, Kondo K, Yang H, Sorokina I, Conaway RC, Conaway JW, Kaelin WG Jr. Biochemical purification and pharmacological inhibition of a mammalian prolyl hydroxylase acting on hypoxia-inducible factor. Proc Natl Acad Sci USA. 2002; 99:13459–13464. [PubMed: 12351678]

Jaiswal M, Sandoval H, Zhang K, Bayat V, Bellen HJ. Probing mechanisms that underlie human neurodegenerative diseases in Drosophila. Annu Rev Genet. 2012; 46:371–396. [PubMed: 22974305]

Joyce JN, Presgraves S, Renish L, Borwege S, Osredkar T, Hagner D, Replogle M, PazSoldan M, Millan MJ. Neuroprotective effects of the novel D3/D2 receptor agonist and antiparkinson agent, S32504, in vitro against 1-methyl-4-phenylpyridinium (MPP+) and in vivo against 1-methyl-4-phenyl-1,2,3,6-tetrahydropyridine (MPTP): a comparison to ropinirole. Exp Neurol. 2003; 184:393–407. [PubMed: 14637109]

Kaur D, Yantiri F, Rajagopalan S, Kumar J, Mo JQ, Boonplueang R, Viswanath V, Jacobs R, Yang L, Beal MF, DiMonte D, Volitaskis I, Ellerby L, Cherny RA, Bush AI, Andersen JK. Genetic or pharmacological iron chelation prevents MPTP-induced neurotoxicity in vivo: a novel therapy for Parkinson's disease. Neuron. 2003; 37:899–909. [PubMed: 12670420]

Kruger R, Kuhn W, Muller T, Woitalla D, Graeber M, Kosel S, Przuntek H, Epplen JT, Schols L, Riess O. Ala30Pro mutation in the gene encoding alpha-synuclein in Parkinson's disease. Nat Genet. 1998; 18:106–108. [PubMed: 9462735]

Lee DW, Rajagopalan S, Siddiq A, Gwiazda R, Yang L, Beal MF, Ratan RR, Andersen JK. Inhibition of prolyl hydroxylase protects against 1-methyl-4-phenyl-1,2,3,6-tetrahydropyridine-induced neurotoxicity: model for the potential involvement of the hypoxia-inducible factor pathway in Parkinson disease. J Biol Chem. 2009; 284:29065–29076. [PubMed: 19679656]

Lei P, Ayton S, Appukuttan AT, Volitakis I, Adlard PA, Finkelstein DI, Bush AI. Clioquinol rescues Parkinsonism and dementia phenotypes of the tau knockout mouse. Neurobiol Dis. 2015; 81:168–175. [PubMed: 25796563]

Li C, Biswas S, Li X, Dutta AK, Le W. Novel D3 dopamine receptor-preferring agonist D-264: Evidence of neuroprotective property in Parkinson's disease animal models induced by 1-methyl-4-phenyl-1,2,3,6-tetrahydropyridine and lactacystin. J Neurosci Res. 2010; 88:2513–2523. [PubMed: 20623619]

Li J, Zhu M, Rajamani S, Uversky VN, Fink AL. Rifampicin inhibits alpha-synuclein fibrillation and disaggregates fibrils. Chem Biol. 2004; 11:1513–1521. [PubMed: 15556002]

Li X, Jankovic J, Le W. Iron chelation and neuroprotection in neurodegenerative diseases. J Neural Transm. 2011; 118:473–477. [PubMed: 21161300]

Marsden CD, Parkes JD. “On-off” effects in patients with Parkinson's disease on chronic levodopa therapy. Lancet. 1976; 1:292–296. [PubMed: 55599]

Modi G, Voshavar C, Gogoi S, Shah M, Antonio T, Reith ME, Dutta AK. Multifunctional D2/D3 agonist D-520 with high in vivo efficacy: modulator of toxicity of alpha-synuclein aggregates. ACS Chem Neurosci. 2014; 5:700–717. [PubMed: 24960209]

Oakley AE, Collingwood JF, Dobson J, Love G, Perrott HR, Edwardson JA, Elstner M, Morris CM. Individual dopaminergic neurons show raised iron levels in Parkinson disease. Neurology. 2007; 68:1820–1825. [PubMed: 17515544]

Olanow CW, Stern MB, Sethi K. The scientific and clinical basis for the treatment of Parkinson disease (2009). Neurology. 2009; 72:S1–136.

Olanow CW, Tatton WG. Etiology and pathogenesis of Parkinson's disease. Annu Rev Neurosci. 1999; 22:123–144. [PubMed: 10202534]

Ostrerova-Golts N, Petrucelli L, Hardy J, Lee JM, Farer M, Wolozin B. The A53T alpha-synuclein mutation increases iron-dependent aggregation and toxicity. J Neurosci. 2000; 20:6048–6054. [PubMed: 10934254]

Pilati N, Barker M, Panteleimonitis S, Donga R, Hamann M. A rapid method combining Golgi and Nissl staining to study neuronal morphology and cytoarchitecture. J Histochem Cytochem. 2008; 56:539–550. [PubMed: 18285350]

Przedborski S, Jackson-Lewis V, Djaldetti R, Liberatore G, Vila M, Vukosavic S, Almer G. The parkinsonian toxin MPTP: action and mechanism. Restor Neurol Neurosci. 2000; 16:135–142. [PubMed: 12671216]

Przedborski S, Tieu K, Perier C, Vila M. MPTP as a mitochondrial neurotoxic model of Parkinson's disease. J Bioenerg Biomembr. 2004; 36:375–379. [PubMed: 15377875]

Rajagopalan S, Rane A, Chinta SJ, Andersen JK. Regulation of ATP13A2 via PHD2-HIF1alpha Signaling Is Critical for Cellular Iron Homeostasis: Implications for Parkinson's Disease. J Neurosci. 2016; 36:1086–1095. [PubMed: 26818499]

Romeo AM, Christen L, Niles EG, Kosman DJ. Intracellular chelation of iron by bipyridyl inhibits DNA virus replication: ribonucleotide reductase maturation as a probe of intracellular iron pools. J Biol Chem. 2001; 276:24301–24308. [PubMed: 11301321]

Rouault TA, Cooperman S. Brain iron metabolism. Semin Pediatr Neurol. 2006; 13:142–148. [PubMed: 17101452]

Santra S, Xu L, Shah M, Johnson M, Dutta A. D-512 and D-440 as novel multifunctional dopamine agonists: characterization of neuroprotection properties and evaluation of in vivo efficacy in a Parkinson's disease animal model. ACS Chem Neurosci. 2013; 4:1382–1392. [PubMed: 23906010]

Schapira A, Bate G, Kirkpatrick P. Rasagiline. Nat Rev Drug Discov. 2005; 4:625–626. [PubMed: 16106586]

Schapira AH, Olanow CW. Neuroprotection in Parkinson disease: mysteries, myths, and misconceptions. JAMA. 2004; 291:358–364. [PubMed: 14734599]

Shah M, Rajagopalan S, Xu L, Voshavar C, Shurubor Y, Beal F, Andersen JK, Dutta AK. The high-affinity D2/D3 agonist D512 protects PC12 cells from 6-OHDA-induced apoptotic cell death and rescues dopaminergic neurons in the MPTP mouse model of Parkinson's disease. J Neurochem. 2014; 131:74–85. [PubMed: 24848702]

Siddiq A, Ayoub IA, Chavez JC, Aminova L, Shah S, LaManna JC, Patton SM, Connor JR, Cherny RA, Volitakis I, Bush AI, Langsetmo I, Seeley T, Gunzler V, Ratan RR. Hypoxia-inducible factor prolyl 4-hydroxylase inhibition. A target for neuroprotection in the central nervous system. J Biol Chem. 2005; 280:41732–41743. [PubMed: 16227210]

Smiley ST, Reers M, Mottola-Hartshorn C, Lin M, Chen A, Smith TW, Steele GD Jr, Chen LB. Intracellular heterogeneity in mitochondrial membrane potentials revealed by a J-aggregate-forming lipophilic cation JC-1. Proc Natl Acad Sci USA. 1991; 88:3671–3675. [PubMed: 2023917]

Soto-Otero R, Mendez-Alvarez E, Hermida-Ameijeiras A, Munoz-Patino AM, Labandeira-Garcia JL. Autoxidation and neurotoxicity of 6-hydroxydopamine in the presence of some antioxidants: potential implication in relation to the pathogenesis of Parkinson's disease. J Neurochem. 2000; 74:1605–1612. [PubMed: 10737618]

Spillantini MG, Schmidt ML, Lee VM, Trojanowski JQ, Jakes R, Goedert M. Alpha-synuclein in Lewy bodies. Nature. 1997; 388:839–840. [PubMed: 9278044]

Szelechowski M, Betourne A, Monnet Y, Ferre CA, Thouard A, Foret C, Peyrin JM, Hunot S, Gonzalez-Dunia D. A viral peptide that targets mitochondria protects against neuronal degeneration in models of Parkinson's disease. Nat Commun. 2014; 5:5181. [PubMed: 25333748]

Tsou WL, Hosking RR, Burr AA, Sutton JR, Ouyang M, Du X, Gomez CM, Todi SV. DnaJ-1 and karyopherin alpha3 suppress degeneration in a new Drosophila model of Spinocerebellar Ataxia Type 6. Hum Mol Genet. 2015a; 24:4385–4396. [PubMed: 25954029]

Tsou WL, Ouyang M, Hosking RR, Sutton JR, Blount JR, Burr AA, Todi SV. The deubiquitinase ataxin-3 requires Rad23 and DnaJ-1 for its neuroprotective role in Drosophila melanogaster. Neurobiol Dis. 2015b; 82:12–21. [PubMed: 26007638]

Uversky VN, Li J, Fink AL. Metal-triggered structural transformations, aggregation, and fibrillation of human alpha-synuclein. A possible molecular NK between Parkinson's disease and heavy metal exposure. J Biol Chem. 2001; 276:44284–44296. [PubMed: 11553618]

Wagner BK, Kitami T, Gilbert TJ, Peck D, Ramanathan A, Schreiber SL, Golub TR, Mootha VK. Large-scale chemical dissection of mitochondrial function. Nat Biotechnol. 2008; 26:343–351. [PubMed: 18297058]

Weinreb O, Mandel S, Youdim MB, Amit T. Targeting dysregulation of brain iron homeostasis in Parkinson's disease by iron chelators. Free Radic Biol Med. 2013; 62:52–64. [PubMed: 23376471]

Winborn BJ, Travis SM, Todi SV, Scaglione KM, Xu P, Williams AJ, Cohen RE, Peng J, Paulson HL. The deubiquitinating enzyme ataxin-3, a polyglutamine disease protein, edits Lys63 linkages in mixed linkage ubiquitin chains. J Biol Chem. 2008; 283:26436–26443. [PubMed: 18599482]

Yedlapudi D, Joshi GS, Luo D, Todi SV, Dutta AK. Inhibition of alpha-synuclein aggregation by multifunctional dopamine agonists assessed by a novel in vitro assay and an in vivo Drosophila synucleinopathy model. Sci Rep. 2016; 6:38510. [PubMed: 27917933]

Yeoh KK, Chan MC, Thalhammer A, Demetriades M, Chowdhury R, Tian YM, Stolze I, McNeill LA, Lee MK, Woon EC, Mackeen MM, Kawamura A, Ratcliffe PJ, Mecinovic J, Schofield CJ. Dual-action inhibitors of HIF prolyl hydroxylases that induce binding of a second iron ion. Org Biomol Chem. 2013; 11:732–745. [PubMed: 23151668]

Zecca L, Youdim MB, Riederer P, Connor JR, Crichton RR. Iron, brain ageing and neurodegenerative disorders. Nat Rev Neurosci. 2004; 5:863–873. [PubMed: 15496864]

Zou L, Xu J, Jankovic J, He Y, Appel SH, Le W. Pramipexole inhibits lipid peroxidation and reduces injury in the substantia nigra induced by the dopaminergic neurotoxin 1-methyl-4-phenyl-1,2,3,6-tetrahydropyridine in C57BL/6 mice. Neurosci Lett. 2000; 281:167–170. [PubMed: 10704769]

A novel multifunctional brain penetrant dopamine D2/D3 agonist D-607 with highly selectivity for chelating to Fe(II) over Fe(III) has been developed.

D-607 exhibits neuroprotection in multiple cellular Parkinson's disease models

D-607 significantly suppressed α-synuclein (α-Syn) induced toxicity in *Drosophila* melanogaster model expressing a disease-causing α-Syn variant of protein in fly eyes

D-607 was able to rescue DAergic neurons from MPTP toxicity in mice, a well-known PD neurotoxicity model, following both sub-chronic and chronic MPTP administration.

The mitochondrial stabilization, inhibition of prolyl hydroxylase domain activity etc. by **D-607** might explain fully or partially mechanism of neuroprotection.

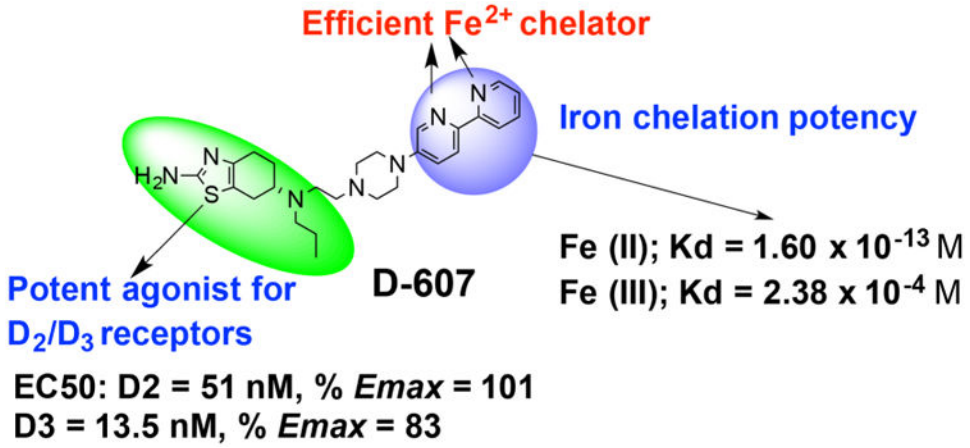

Fig. 1.

Molecular structure of **D-607** with illustration of dopamine agonist and iron chelating properties (Das et. al. *ACS Chem Neurosci, 2017*).

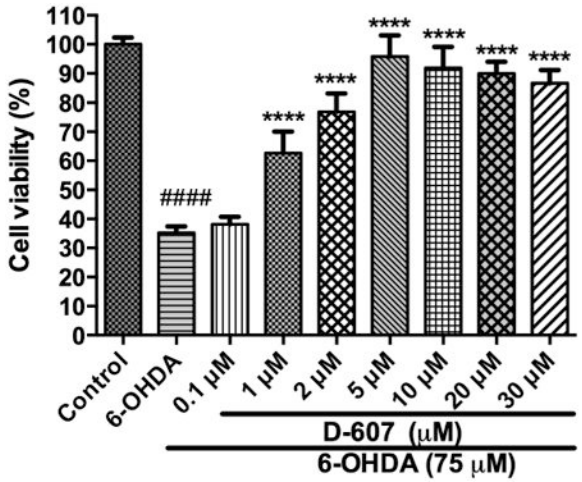

Fig. 2.

Dose-dependent effect of **D-607** on cell viability of PC12 cells from toxicity induced by 75 μM 6-OHDA. PC12 cells were pre-treated with varying concentrations of **D-607** for 1 h after which the media was replaced with fresh culture media followed by treatment with 75 μM 6-OHDA for another 24 h. The values shown are the mean ± SD of at least three independent experiments performed in four to six replicates. One way ANOVA analysis $F(8, 62) = 160.8$, $p < 0.0001$. ANOVA was followed by Tukey's multiple comparison post hoc test (****$p < 0.0001$ compared to 6-OHDA only and ####$p < 0.0001$ compared to control).

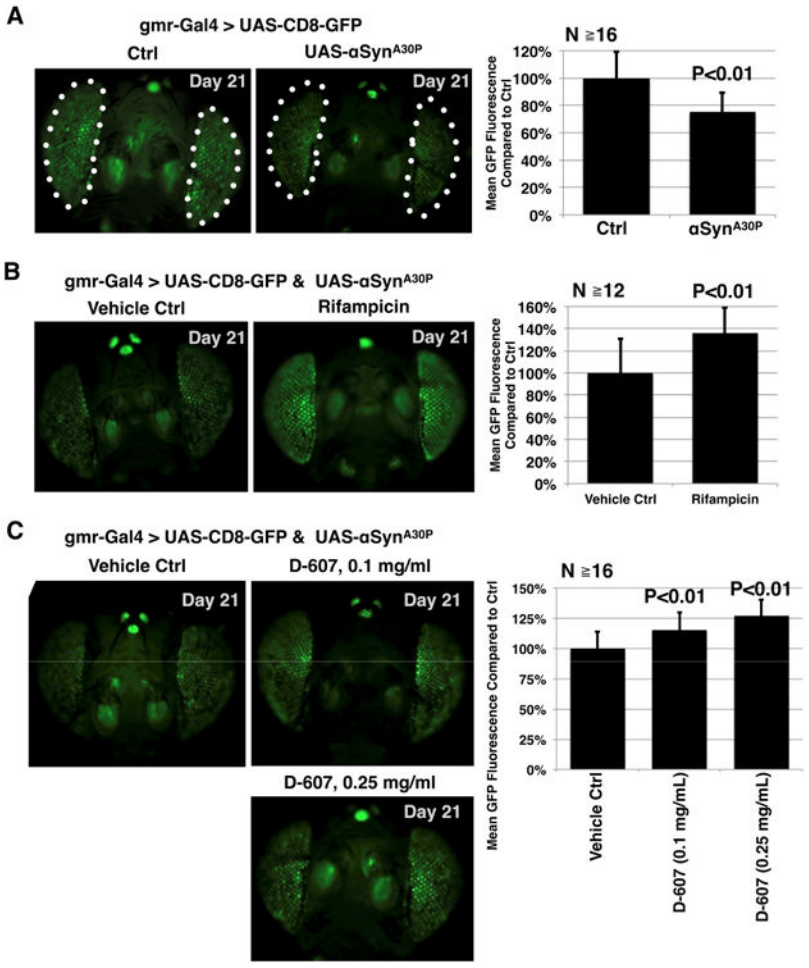

Fig. 3.

Compound **D-607** suppresses toxicity from α-Syn in fly eyes. (A) Left: fluorescent images of control fly eyes or eyes expressing UAS-α-SynA30P driven by GMR-Gal4. Flies were heterozygous for the transgenes. Ctrl: GMR-Gal4 on the isogenic background of the UAS-α-SynA30P line. Dotted lines: fly eyes, which were quantified in the right panel. Right: Quantification of data from the left and other flies of the same genotype. Shown are means -/+ standard deviations. P value is from Student's T-test, compared to the control group. (B) Left: fluorescent images of fly eyes expressing UAS-α-SynA30P driven by GMR-Gal4 that were fed the vehicle control (DMSO) or rifampicin (1mg/ml) for 21 days. Flies were heterozygous for the transgenes. Right: Quantification of data from the left and other flies of the same genotype. Shown are means -/+ standard deviations. P value is from Student's T-test. (C) Left: fluorescent images of fly eyes expressing UAS-α-SynA30P driven by GMR-Gal4 that were fed the vehicle control (water) or compound **D-607** for the indicated days and at the noted concentration. Flies were heterozygous for the transgenes. Right: Quantification of data from the left and other flies of the same genotype. P values are from ANOVA followed by Tukey's multiple comparison post hoc test.

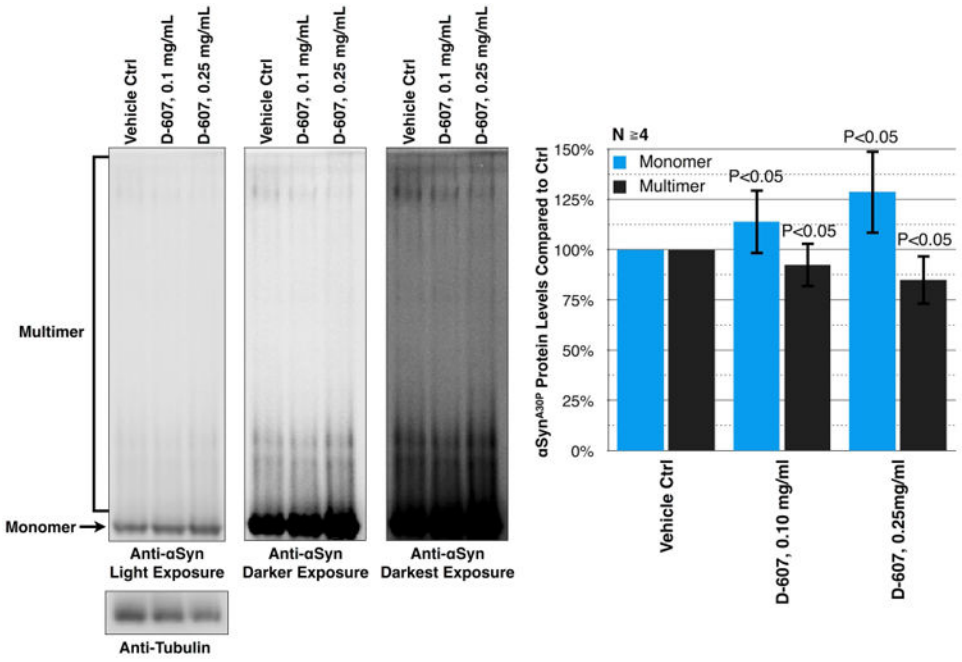

Fig. 4.

Left: Shown are western blots of native gels from dissected fly heads that express α-Syn (A30P) in their eyes, treated, or not, with compound **D-607** for 21 days at the noted concentration. These heads are the same as the ones that were imaged and used for quantification in Fig. 3. Monomeric (arrow) and multimeric/aggregated α-Syn (entire bracket) species are noted on the left of the blot. Three different exposures of the same membrane are shown to highlight soluble and aggregated species of α-Syn. Right: Histograms show levels of monomeric and multimeric α-Syn, compared to the vehicle control. For quantification, the signal intensity of monomeric and multimeric α-Syn of each individual lane was divided by the total signal of α-Syn (monomeric + multimeric) for that specific lane. For the monomeric species, we focused on the band highlighted by the arrow. For the multimeric species, we quantified the signal from the entire, bracketed area. The resulting values were divided by the total α-Syn signal for each lane, and then were compared to the control lane, which was set to 100%. P values are from Student's t-tests, comparing **D-607**-treated flies to vehicle control ones.

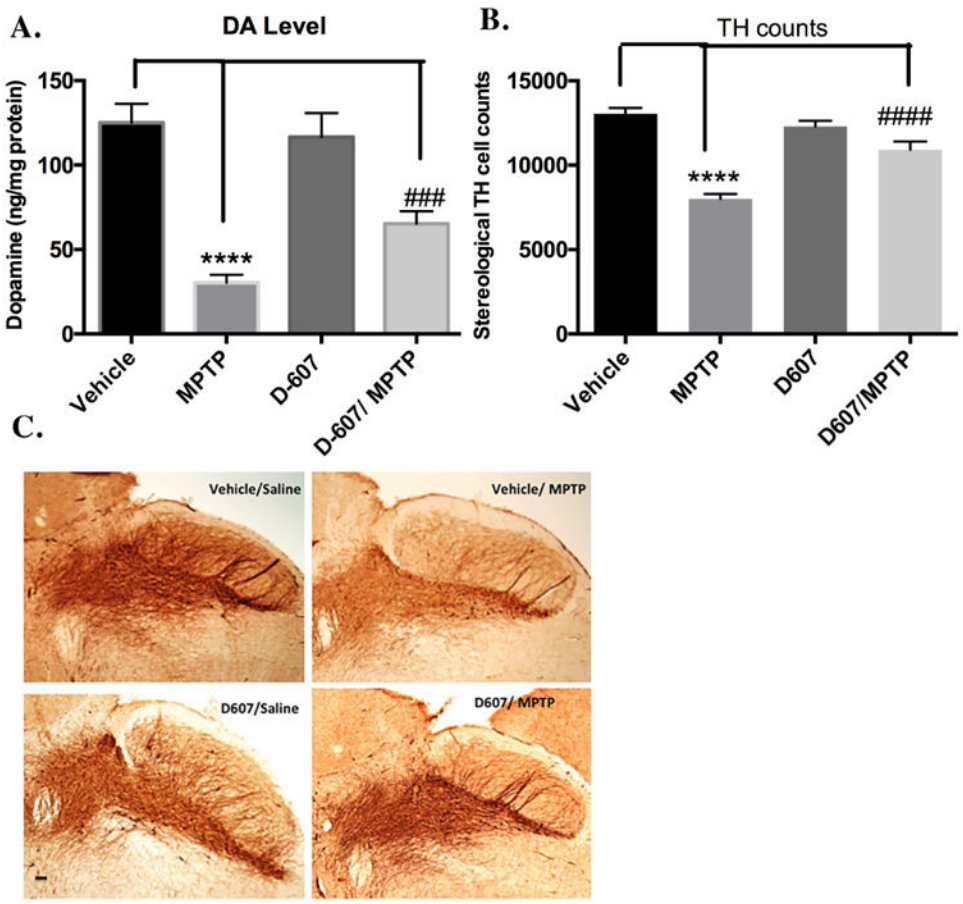

Fig. 5.

A. (a) Effect of pre-treatment with 5 mg/kg **D-607** for three days followed by two days co-treatment with MPTP (20 mg/kg, 12 h apart) on striatal DA levels. One way ANOVA analysis ($F(3, 16) = 97.71$, $p < 0.0001$) **** $p < 0.0001$ between vehicle/Sal and Vehicle/MPTP; ### $p<0.001$ between **D-607**/MPTP and Vehicle/MPTP (n=6). **B.** Stereological quantification of TH-positive DAergic cell counts within the SNpc. One way ANOVA analysis ($F(3, 16) = 179.9$, $p < 0.0001$) indicates **** $p < 0.0001$ between Vehicle/Sal and Vehicle/MPTP; #### $p < 0.0001$ between **D-607**/MPTP and Vehicle/MPTP with **D-607** at 5 mg/kg concentration (n=6). **C.** Representative photomicrographs of the SN with TH immunohistochemistry (10×).

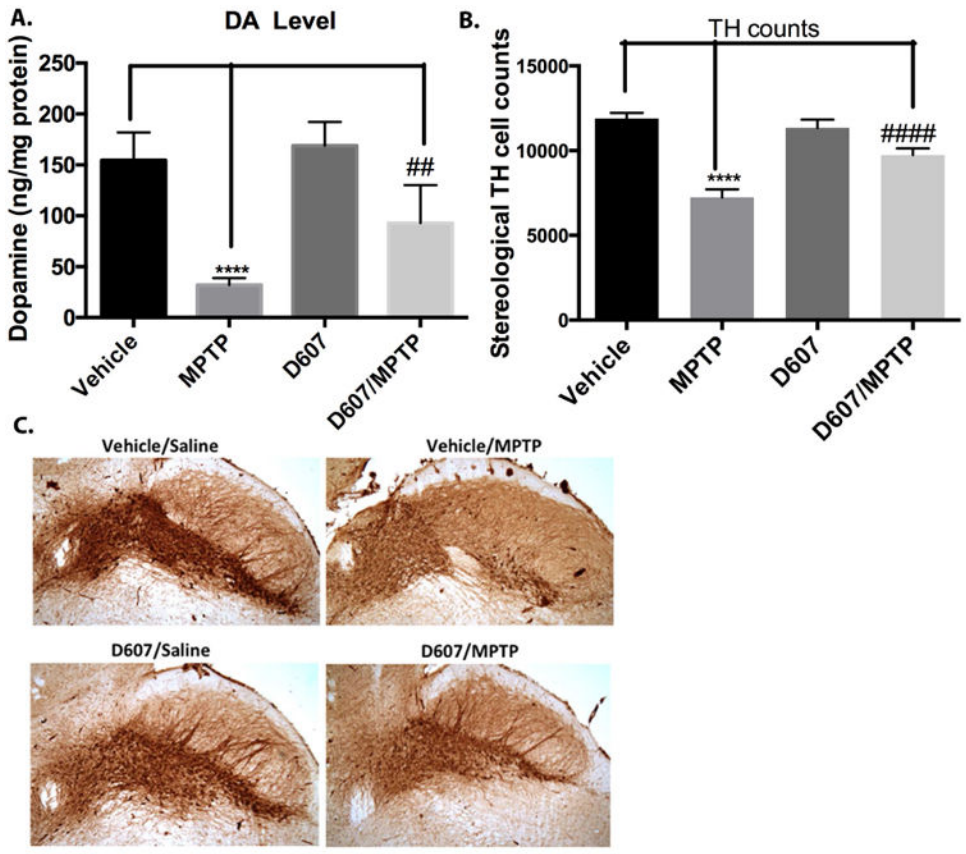

Fig. 6.

A. (a) Effect of pretreatment of 5 mg/kg **D-607** for three days followed by five days co-treatment with MPTP (20 mg/kg, 24 h apart) on striatal DA levels. One way ANOVA analysis (F3, 20) = 34.61 $p < 0.0001$) ****$p < 0.0001$ between vehicle and MPTP; ##$p < 0.01$ between D-607/MPTP and MPTP for DA levels. (n=6). **B.** Stereological quantification of TH-positive DAergic cell counts within the SNpc. One way ANOVA analysis (F (3, 20) = 144.5, $p < 0.0001$) indicates ****$p < 0.0001$ between vehicle and MPTP; ####$p < 0.0001$ between D-607/MPTP and MPTP (n=6). **C.** Representative photomicrographs of the SN with TH immunohistochemistry (10×).

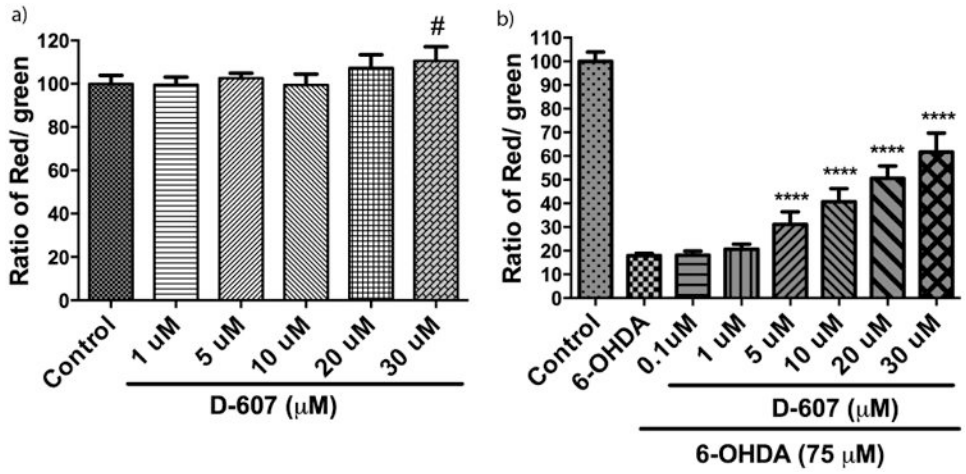

Fig. 7.

Effect of **D-607** on 6-OHDA induced mitochondrial membrane potential (MMP) loss. **a)** PC12 cells were treated with various concentrations (1, 5, 10, 20 and 30 μM) of **D-607** for 24 h and JC-1 staining was carried out. **b)** PC12 cells were treated with various concentrations (0.1, 1, 5, 10, 20 and 30 μM) of **D-607** for 1 h followed by treatment with 6-OHDA (75 μM) for a period of 24 h. Graphs showing the ratio of JC-1 red fluorescence to green fluorescence have been plotted and loss of MMP was demonstrated by the change in JC-1 fluorescence from red (JC-1 aggregates) to green (JC-1 monomers). Data represents mean ± SD of 3 independent experiments. One way ANOVA analysis $F(5, 22) = 4.45$, $p < 0.01$ for 7a, $F(7, 56) = 286.5$, $p < 0.0001$ for 7b. ANOVA was followed by Tukey's multiple comparison post hoc test (#$p< 0.05$ compared to control, ****$p< 0.0001$ compared to 6-OHDA alone).

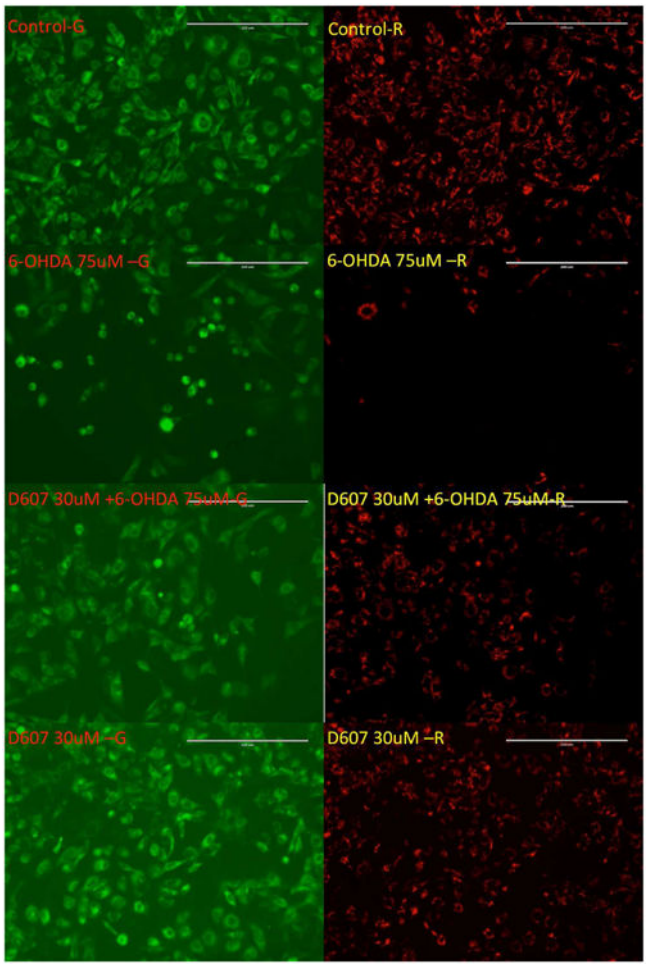

Fig. 8.

Effect of **D-607** on mitochondrial membrane potential loss induced by 6-OHDA. PC12 cells were treated with either 30 μM **D-607** or 75 μM 6-OHDA alone, as well as 30 μM **D-607** for 1 h followed by treatment with 75 μM 6-OHDA for a period of 24 h. Controls received DMSO only. JC-1 staining was carried out and the images showing the JC-1 aggregates under the rhodamine filter and JC-1 monomers under FITC filter were taken using fluorescent microscope under 20× magnification.

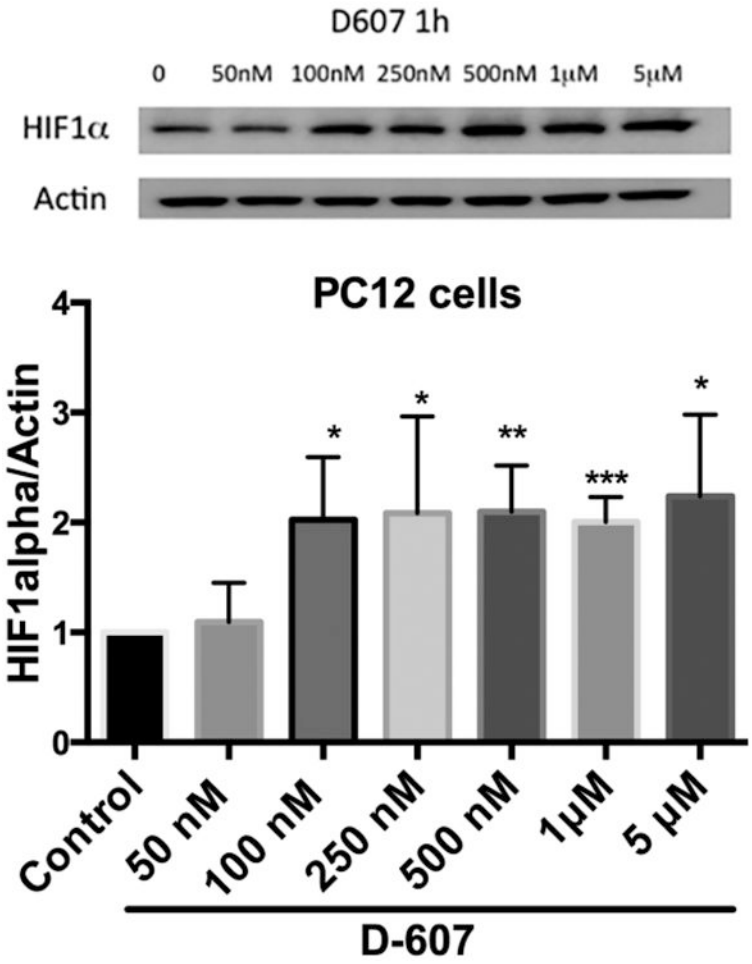

Fig. 9.

Dose dependent effect of **D-607** on cellular HIF-1α levels. Western blot analysis was used to follow HIF-1α relative to actin expression as described under materials and methods section. Results are representative of three individual experiments. Student t-test analysis of each treatment group to control, ***$p < 0.0001$, **$p < 0.001$ and *$p<0.01$ compared to control.